DOKTORSAVHANDLINGAR
VID
CHALMERS TEKNISKA HÖGSKOLA
Nr 118

CONTRIBUTIONS TO RADIO ASTRONOMY AND ELECTROMAGNETIC WAVE THEORY

Microwave Observations of Galactic OH, and Very High Resolution Interferometry. Distortion of Electromagnetic Wave Trains in Ionized Media

BY

BERNT O. RÖNNÄNG

GÖTEBORG 1972

CONTRIBUTIONS TO RADIO ASTRONOMY AND ELECTROMAGNETIC WAVE THEORY

Microwave Observations of Galactic OH, and Very High Resolution Interferometry. Distortion of Electromagnetic Wave Trains in Ionized Media

AKADEMISK AVHANDLING

SOM MED TILLSTÅND AV CHALMERS TEKNISKA HÖGSKOLA
FÖR TEKNOLOGIE DOKTORSGRADS VINNANDE TILL
OFFENTLIG GRANSKNING FRAMLÄGGES Å PALMSTEDTSALEN
INOM KANSLIBYGGNADEN, SVEN HULTINS GATA, GÖTEBORG,
FREDAGEN DEN 10 NOVEMBER 1972, KL. 10.00

AV

BERNT O. RÖNNÄNG

Teknologie licentiat

AVHANDLINGEN FÖRSVARAS PÅ ENGELSKA OCH SVENSKA SPRÅKET

GÖTEBORG
ELANDERS BOKTRYCKERI AKTIEBOLAG
1972

DOKTORSAVHANDLINGAR
VID
CHALMERS TEKNISKA HÖGSKOLA

CONTRIBUTIONS TO RADIO ASTRONOMY AND ELECTROMAGNETIC WAVE THEORY

Microwave Observations of Galactic OH, and Very High Resolution Interferometry. Distortion of Electromagnetic Wave Trains in Ionized Media

BY

BERNT O. RÖNNÄNG

GÖTEBORG
ELANDERS BOKTRYCKERI AKTIEBOLAG
1972

The present paper serves as an introduction to and a summary of a doctoral thesis which includes the following papers:

A. J. Elldér, B. O. Rönnäng, A. Winnberg, "New OH Radio Emission Sources in Cygnus", Nature, *222*, 67–69, (1969).

B. T. Cato, J. Elldér, B. Höglund, O. E. H. Rydbeck, B. O. Rönnäng, A. Sume, "Searches for Microwave Spectral Line Radiation from Some Molecules in the Interstellar Medium", Research Report No. 109, Research Laboratory of Electronics, Chalmers University of Technology, (1972).

C. B. O. Rönnäng, "High Resolution Spectra of Some Strong Galactic OH Emission Sources", Research Report No. 101, Research Laboratory of Electronics, Chalmers University of Technology, (1972).

D. B. O. Rönnäng, O. E. H. Rydbeck, J. M. Moran, "Very Long Baseline Interferometry of Galactic OH Sources", Radio Science, *5*, 1227–1231, (1970).

E. B. O. Rönnäng, "On the Theory, Techniques, and Data Processing of Very Long Baseline Interferometry", Research Report No. 105, Research Laboratory of Electronics, Chalmers University of Technology, (1971).

F. K. I. Kellermann, D. L. Jauncey, M. H. Cohen, D. B. Shaffer, B. G. Clark, J. Broderick, B. O. Rönnäng, O. E. H. Rydbeck, L. Matveyenko, I. Moiseyev, V. V. Vitkevitch, B. F. C. Cooper, R. Batchelor, "High-Resolution Observations of Compact Radio Sources at 6 and 18 Centimeters", Ap.J., *169*, 1–24, (1971).

G. B. O. Rönnäng, "Transient Wave Propagation in Inhomogeneous Ionized Media", Research Report No. 70, Research Laboratory of Electronics, Chalmers University of Technology, (1966).

H. B. O. Rönnäng, "Signal Distortion in Anisotropic Homogeneous Ionized Media. 1. Longitudinal Magnetic Field", Research Report No. 73, Research Laboratory of Electronics, Chalmers University of Technology, (1967).

INTRODUCTION

The present thesis combines two fields within physics and engineering:

1. Radio astronomy, mainly dealing with observations of spectral line emission from the hydroxyl radical (OH), searches for other molecules in the Galaxy, and very long baseline interferometer (VLBI) measurements.
2. Theoretical work on electromagnetic wave propagation in dispersive media, mainly dealing with the distortion of pulses propagating in plasmas or waveguides.

1. **Radio astronomy**

Microwave radiation from interstellar hydroxyl (OH)

The first spectral line detected by radio astronomers was the one at 1420 MHz due to neutral hydrogen. It was discovered in 1951 after its detectability had been predicted by van der Hulst in 1945. This was one of the greatest breakthroughs in radio astronomy. The line profiles of the most abundant element in interstellar space have facilitated measurement of the differential motion and the spiral structure of the Galaxy.

For a long time the neutral hydrogen line remained the only known radio spectral line. Proposals regarding the detectability of many others were made. Shkovskij was the first to suggest that the lambda doublet lines of simple diatomic molecules, such as OH and CH might be detected. In 1963 the spectral lines of the hydroxyl radical (OH) at 1665 MHz and 1667 MHz were discovered in absorption against the radio source Cas. A (S. Weinreb *et al.*, 1963) and two years later OH in emission was detected by groups at Harvard and Berkeley.

The four electric dipole transitions of OH in the radio spectrum at frequencies 1612, 1665, 1667, and 1720 MHz are due to energy level splitting of the ground state $^2\Pi_{3/2}$, $J=3/2$, first by lambda doubling and then by hyperfine splitting. Under local thermodynamic equilibrium conditions (and small optical depth) the intensity ratios of the observed four OH lines should be 1:5:9:1. However, in most cases the observed intensity ratios are found not to conform with the conditions of thermodynamic equilibrium. Various processes of populating the four levels have been proposed.

Interstellar OH has been observed both in absorption and emission. Essen-

tially every continuum source in the galactic plane that has been searched for OH shows absorption lines. The interstellar clouds producing OH are strongly concentrated towards the galactic plane and are presumed to be distributed in the spiral arms of the Galaxy much like the neutral hydrogen.

OH in emission was detected in the direction of several emission nebulae. In most cases the OH emission lines are very narrow in frequency and exhibit complicated polarization effects, high brightness temperatures, and intensity fluctuations. These characteristics are evidence of a non-thermal population distribution of the molecular states, corresponding to a population inversion and hence maser action. Most sources of anomalous OH emission have been detected in the immediate vicinity of H II regions and many of them have been shown to be associated with very compact H II regions. However, several non-thermal sources and infrared (IR) stars have been observed to show intense OH emission. The anomalous OH emission sources are usually divided into two classes depending on the frequency of the strongest emission feature. Class I corresponds to the most intense emission in the main lines (1665 and 1667 MHz) and class II corresponds to the most intense emission in the satellite lines [II (*a*) at 1720 MHz, II (*b*) at 1612 MHz]. To a significant extent the differentiation by class seems to reflect the difference in the origin of the emission. Most OH emission sources associated with H II regions belong to class I; most sources associated with non-thermal sources (supernova remnants) belong to class II (*a*); and all sources associated with IR stars belong to class II (*b*).

The early conclusion that most OH emission sources are associated with H II regions could be biased because the search was concentrated on thermal continuum sources. The discovery of intense OH emission from two IR stars by Wilson and Barret in 1968 inspired us to perform the unbiased search for OH emission sources in the Cygnus direction which is reported in paper A. Four new sources emitting strong OH radiation were detected and all three classes of emission sources were represented.

Interferometer measurements with longer and longer baselines failed to resolve the OH emission sources. It was not until the new techniques of very long baseline interferometry (described on pages 6–9 and in paper E) were used that the structure of some of the most intense sources was revealed. Such measurements were performed in 1968 with Onsala Space Observatory as one of the stations in a famous four station experiment (Moran *et al.*, 1968). New measurements, performed in July 1969, are reported in paper D. These two-station observations with a baseline 5600 km (31.1×10^6 wavelengths) long confirmed the size and structure of the OH emission source near the radio source W3 and gave additional information on the complex structure of the various features. Four other galactic OH emission sources with unknown sizes were also investigated.

Typical sizes of individual OH emission sources are in the range 0.005 to

0.05 arc sec. The apparent physical size of the smallest sources is then of the order of a few astronomical units. However, there are those who believe that the true source size may be much smaller as the apparent size may be due to scattering of the 18-cm radiation by irregularities in the free electron density in the interstellar medium. Other mechanisms have also been proposed which dissolve the relation between the observed angular dimension and the true physical size.

The VLBI observations reveal that the bright features in the overall emission spectra originate from separate emission sources. This fact, and the uncertainty regarding the geometric models and pumping mechanism of the OH maser, stress the necessity of detailed observations of the OH spectra. Paper C describes observations of this kind where the 84-foot telescope of the Onsala Space Observatory was used to measure the spectra of eight well-known strong OH sources. 250 Hz frequency resolution was used and the spectra were decomposed into Gaussian components in order to study the shape (and possible time variations in intensity, line width, and radial velocity) of the individual features. It is well-known that an unsaturated masering OH cloud should give rise to a spectral line of exponential Gaussian form and that an intensity change should be followed by a change in line width.

Microwave radiation from other molecules in interstellar space

The neutral hydrogen radiation was detected in 1951 and the OH molecule radiation in 1963. As of today, the existence of more than twenty different molecules (and some of their isotopic species) in interstellar space has been established (Rank *et al.*, 1971). A picture of a surprisingly complex chemistry is beginning to emerge and will, no doubt, be considerably extended during the next few years.

The various molecular transitions occur in characteristic regions of the spectrum and in the frequency range below 10 GHz the fine structure, hyperfine structure, and lambda and K doubled transitions are most important. A few criteria ought to be fulfilled before a search for a new molecular line starts. The molecule, or at least the elements forming the molecule must be present in sufficient amount in the interstellar medium. A transition must be found which has a known frequency and a high transition probability. Finally, the transition must be close enough to the ground energy state to ensure that the levels are significantly populated. Paper B summarizes the searches at the Onsala Space Observatory for absorption or emission lines from a number of different organic and inorganic molecules in the direction of several radio sources. The molecules include OH (the vibrationally excited $^2\Pi_{3/2}$, $J=3/2$, $v=1$ state), CH, SO_2, HCN, H_2CS, NH_2CHO, and CH_3CHO. All searches gave negative results, for the molecular states in question, with the possible exception of H_2CS (in the radio source W51).

Very long baseline interferometry

The ability of a telescope to resolve small scale structure increases as the size of the instrument is increased but decreases with increasing wavelength. This explains why even the largest radio telescopes have only about the resolving power of the human eye—one thousand times poorer resolution than that of the largest optical telescope. The radio interferometer, where two or more widely spaced radio telescopes are connected to a single receiver, is the instrument to overcome this fundamental difficulty.

The principle of the interferometer was first used in optical astronomy in 1920 by Michelson (1920) to measure the diameter of stars. However, the Michelson interferometer was extremely difficult to handle and the observational results are very uncertain. The history of radio interferometry goes back to 1946, when McReady *et al.* (1947) started solar observations with the cliff interferometer at Sydney. The more conventional two-element interferometer also came into use in 1946, with solar observations by Ryle and Vonberg (1946) at Cambridge. Both these instruments operated at a wavelength near 1.5 m and had a resolution of about 10 arc min.

For small separations, a few km or less, the antennas may be connected to the common receiver by microwave cables. For longer separations the use of cables becomes impractical. However, microwave links can replace the cables and extend the maximum baseline length to a few hundred km. The most powerful microwave link interferometer is the Jodrell Bank one, which by 1965 had been used with a baseline 127 km long. At the shortest wavelength used so far (6 cm) this baseline results in a fringe spacing of 0.1 arc sec.

Table I. Comparative resolving power

Instrument	Wavelength (cm)	Diameter or aerial separation (m)	Approximate resolution (arc sec)
Human eye	0.00005	0.003	60
84-foot radio telescope	6	25.6	600
200-inch Palomar telescope	0.00005	5.1	0.03*
Michelson interferometer (1920)	0.00005	6.0	0.02
Australian cliff interferometer (1946)	150	—	600
Hanbury Brown & Twiss (Narrabri) interferometer	0.000044	188	0.0005
Jodrell Bank radio interferometer (1965)	6	$127 \cdot 10^3$	0.03
The very long baseline interferometer (1969)	6	$10536 \cdot 10^3$	0.0004

* Theoretical limit. The resolution of a filled aperture telescope is, in fact, limited by irregularities in the earth's atmosphere to about one arc second.

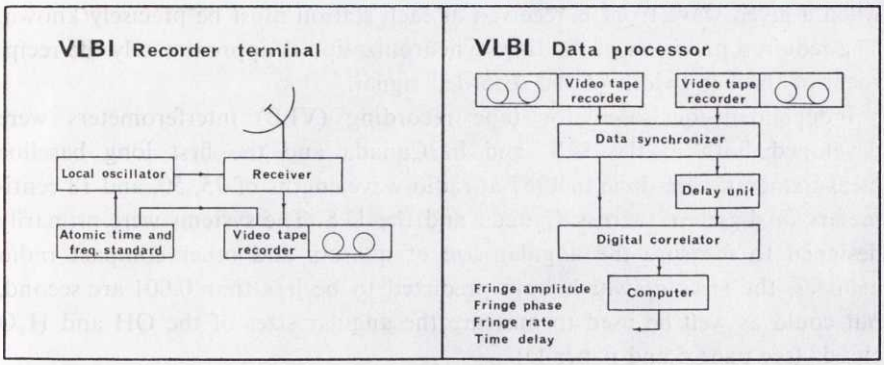

Fig. 1. The very long baseline interferometer makes it possible to do interferometry with radio telescopes almost as far apart as opposite sides of the earth. The signals from each antenna are separately recorded at each end of the interferometer system, and later the magnetic tapes are transported to the National Radio Astronomy Observatory in the United States or to the Onsala Space Observatory where recorded data are correlated in a special purpose computer.

The operation of a radio interferometer is absolutely dependent on phase stability of the receivers, which must for most purposes be maintained to within a few electrical degrees, and this becomes difficult as the separation between the antennas increases. (The Hanbury Brown and Twiss intensity interferometer built in 1956 had disposed of the common local oscillator requirement, but at the cost of a severely reduced sensitivity). It therefore appears unlikely that the baseline of the Jodrell Bank interferometer can be extended appreciably. The next step would then be to eliminate all real-time interconnections which means that there will no longer be any limitation on the separation of the stations. This is the definition of a very long baseline interferometer (VLBI).

Three main requirements must be considered in the development of the VLBI system. First, the signal must be stored somewhere, for example on magnetic tapes, and in that case the tape recorders have to be capable of recording a wide band of frequencies and of faithfully reproducing them on playback.

The second major requirement concerns the local oscillators at the two ends of the baseline. The local oscillators must have relative stabilities at least of the order of one part in 10^{11}. Atomic frequency standards possess this high degree of stability. Future VLBI-measurements, especially for geodetic purposes, will undoubtedly require even higher local oscillator stabilities and thus, in extreme cases, even the use of hydrogen maser standards. The Onsala Observatory will be equipped with such a standard in 1973.

The third major requirement arises when the tapes are played back. The time

when a given wave front is received at each station must be precisely known. The required precision of the time synchronization is approximately the reciprocal of the bandwidth of the recorded signal.

Independent-local-oscillator tape recording (VLB) interferometers were developed both in the U.S. and in Canada and the first long baseline measurements were done in 1967 at radio wavelengths of 75, 50, and 18 centimeters on baselines across Canada and the U.S. The systems were primarily designed to measure the angular size of quasars and other compact radio galaxies, the sizes of which were predicted to be less than 0.001 arc second, but could as well be used to measure the angular sizes of the OH and H_2O clouds (see page 4 and paper D).

The Onsala VLBI system, described in paper E, was developed in 1969 and is similar to the U.S. system. While the Canadian group uses analogue techniques the American system records the signal digitally on the magnetic tapes. This technique narrows the frequency band which can be recorded, but this disadvantage is balanced by the advantage inherent in digital systems.

As of today the second generation of complete VLBI systems is developed, one system at the National Radio Astronomy Observatory in the U.S. and another at the Onsala Space Observatory (to be fully completed in 1973). These systems allow a frequency band of 2 MHz to be recorded and include a special purpose computer for data reduction, and hydrogen maser oscillators. Their use will open exciting applications of the long baseline interferometer in such diverse fields as astronomy, physics and geodesy. For example, it should be possible to determine relative source positions to better than 0.001 arc sec. The accurately determined positions could then form a reference system for determining the relative positions of the telescopes, to synchronize clocks over intercontinental distances, to look for continental drifts, and to study the motion of the axis of rotation of the earth. The VLBI technique has, of course, also future applications in planetary space science.

A few words ought to be said about future VLBI systems. Will the baselines continue to extend into space, to the moon and beyond? Just as turbulence in the atmosphere affects optical astronomy, so at short wavelengths it will affect radio astronomy. For measurements made at longer wavelengths the scattering of radio waves by electrons in the solar wind and in the interstellar medium limits the angular resolution. Furthermore, there is a fundamental reason (see paper F) why the maximum baseline needed to resolve synchrotron sources, like the quasars, is comparable to the diameter of the earth. Therefore the trend will probably not be towards further extension of the baseline length. Many baselines of intermediate length are also required to give a complete picture of a complex radio source. A global long-baseline interferometer network ought to be constructed. The opportunities such a very long baseline array would provide for both astrophysics and geophysics are enormous.

In January 1968 the first intercontinental interferometric measurements of quasars and radio galaxies were made with the 84-foot telescope of the Onsala Space Observatory and the 140-foot telescope at Green Bank, National Radio Astronomy Observatory (Kellermann *et al.*, 1968) at wavelengths of 18 cm and 6 cm. New measurements made during 1969 with stations in the United States, Australia, U.S.S.R. and the Onsala Observatory are reported in paper C. Many sources, including optically identified galaxies and quasars, are found to have several distinct components of widely differing sizes in the range from a few hundreths of an arc second to the limit of the actual resolution (0.0004 arc sec). One component in the Seyfert galaxy 3C 84 showed an apparent increase in angular size of about 35 per cent in one year. Table II lists all the baselines used.

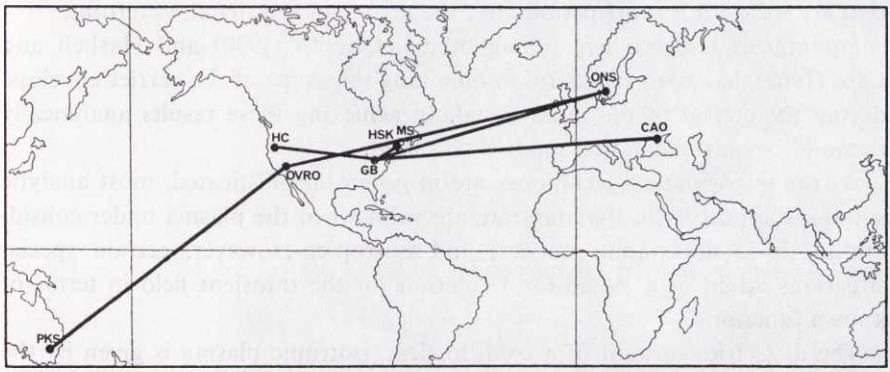

Table II. Some interferometer baselines used to study compact radio sources[1]

Baseline[2]	λ (cm)	Separation (km)	Separation ($10^6\lambda$)	Dates
GB-HSK, GB-MS	18	845	4.7	1967 July and August, 1968 April
GB-HC	18	3 500	19.4	1967 August
GB-ONS	18	6 319	35.1	1969 April II
GB-ONS	6	6 319	105	1969 January II
GB-OVRO	6	3 324	55.5	1969 January, March, April, May
OVRO-ONS	6	7 914	132	1969 February
OVRO-PKS	6	10 536	176	1969 April
GB-CAO	6	8 035	134	1969 October

[1] The results are reported in paper F.

[2] GB=Green Bank, National Radio Astronomy Observatory. HSK=Haystack Microwave Facility, MIT-Lincoln Lab. MS=Millstone, MIT-Lincoln Lab. HC=Hat Creek, Univ. of California, Berkeley. ONS=Onsala Space Observatory, Chalmers Univ. of Techn. OVRO=Owens Valley Radio Observatory, Caltech. PKS=Parkes, Australian National Radio Observatory. CAO=Crimean Astrophysical Observatory.

2. Electromagnetic wave theory

The theory of electromagnetic wave propagation in dispersive media has been developed mainly for time-harmonic fields. However, the propagation of transient signals in dispersive media has received increased attention recently because of its relevance to pulsed excitation of waveguides, whistler propagation in magnetospheric ducts, ionospheric and VLF propagation problems, plasma diagnostics, etc. Pulse distortion is also of interest in the problem of optimizing signal detection at the receiver.

Many studies have been concerned with the distortion that the envelope of a propagating electromagnetic wave train suffers due to the dispersive nature of a plasma. As the problem is exceedingly complex for all but a few cases, early investigators such as Sommerfeld and Brillouin[1] (1914) obtained solutions that are valid for a short period after the arrival of the signal wavefront.

Subsequent research by, among others, Cerrillo (1950) and Haskell and Case (1967), has been successful in obtaining the shape of the carrier envelope during the arrival of the main signal. In achieving these results analytically the saddle-point integration method was used.

As the mathematical techniques are in general sophisticated, most analytic solutions appearing in the literature are valid when the plasma under consideration is lossless, homogeneous, and isotropic. However, certain special situations admit of a closed-form solution for the transient field in terms of known functions.

The dielectric constant of a cold, lossless, isotropic plasma is given by the relation

$$\varepsilon(\omega)=\varepsilon_0(1-\omega_p{}^2/\omega^2) \tag{1}$$

where $\omega_p=(N_0e^2/m\varepsilon_0)^{1/2}$ is the plasma angular frequency and N_0 is the electron density.

In the simple case of a semi-infinite, homogeneous plasma (or waveguide) the unit step wave response (the transmitted and reflected electromagnetic fields, assuming an incident unit step wave) can be written as the sum of two Bessel functions and the unit step modulated carrier response as the sum of two Lommel functions.

If the plasma is inhomogeneous electromagnetic pulse propagation is more complicated. Two cases are studied in paper G where it is shown that the unit step wave response can be expressed as a Bessel function when the electron density profile of a plane, lossless, isotropic, ionized medium (plasma) varies exponentially in one direction, and as a Legendre function if the electron density profile varies in the Epstein layer fashion. It is notable that the Epstein

[1]) The early work by Sommerfeld and Brillouin was initiated by the discussion of group velocity contra signal velocity in dispersive media.

layer is a good approximation to the earth's ionosphere, the electron density profile of which is normally examined by ground based or top-side radar pulse (sounding) techniques.

The ionosphere is anisotropic due to the magnetic field of the earth. A plane polarized electromagnetic wave propagating along the magnetic field will therefore be split into two propagation modes representing the left circularly and the right circularly polarized wave components. A simplified case is treated in paper H, where the transient decomposition of a pulse into two pulses in an anisotropic, homogeneous plasma is treated.

PAPER A

New OH Radio Emission Sources in Cygnus

Theories for the anomalous excitation of galactic OH have been guided by the observed association of the various types of anomalous emission with certain types of astronomical objects. The principal surveys by Weaver *et al.* (1968), and Goss (1968) stressed the association with the brighter HII regions and nonthermal radio sources. However, Raimond and Eliasson (1967) found that the 1665 MHz OH emission of Orion A coincided very accurately with the infrared point source discovered by Becklin (Becklin and Neugebauer, 1967), and further Wilson and Barret (1968) discovered 1612 MHz line emission from four extremely red objects described by Neugebauer *et al.* (1965) and by Ulrich *et al.* (1966).

The search for OH emission sources performed in 1968 and reported in Paper A was inspired by the discovery made by Wilson and Barret. We suspected that the earlier conclusion that most OH emission sources are associated with HII regions might be a selection effect. An unbiased search of a strip of the sky without any preassumtions might reveal such a selection effect.

The main points of paper A are the following:

1. The observations were made with the Onsala 84-foot antenna, equipped with a travelling wave maser and a 100 channel spectral line receiver.

2. A narrow strip within about $\pm 1.5°$ of the galactic equator was searched. The Cygnus direction was initially chosen because it is tangential to the local spiral arm. The galactic longitude interval between $l=68°$ and $l=92°$ was covered. The points of observation within the area were separated by 0.5° in both right ascension and declination. The area was searched at 1665 and 1612 MHz with a right circularly polarized antenna. The sensitivity of the measurements was about 0.5°K antenna temperature averaged over 10 kHz.

3. Four new OH sources were discovered. Their positions were carefully measured and given as equatorial coordinates, epoch 1950.0, and galactic coordinates. The kinematic distances were calculated from the average radial velocity of the sources and the differential galactic rotation model given by Schmidt (1965). Spectra of the OH lines for the different sources are presented.

Sources No. 1 and No. 2 are strongest in the 1665 and 1667 MHz lines. Source No. 3 is strongest at 1720 and source No. 4 at 1612 MHz.

4. The National Geographic—Palomar Observatory Sky Survey plates were examined for possible identifications. The region around source No. 1 was found to be heavily obscured and no HII-region or other conspicuous object was found. A few stars were seen which are only visible on the red-sensitive plate, but it might well be that these are luminous, highly reddened stars. No continuum radiation was detected stronger than 0.2°K antenna temperature.

The area around source No. 2 seemed to have an even higher absorption than the area around source No. 1. Therefore, there are many red stars in the area which are probably reddened by dust. A small maximum of continuum radiation ($T_A \approx 3.5°$ K) was detected at the source position.

Source No. 3 lies in an area with a very high field density of stars. Two small H II regions can be seen.

In the area of source No. 4 an extended weak H II-region with central obscuring dust clouds can be seen. The OH source lies in the eastern part of this nebula. There is one star close to source No. 4 which can only be seen on the red-sensitive plate. The estimated coordinates of this star are given.

The suspicion of a selection effect proved to be true. The four new sources represented all three classes of OH emission sources [according to the classification made later by Turner (1969)]. A short summary of subsequent work regarding the ON 1–4 sources by Wynn-Williams (1969), Winnberg (1970), Hardebeck (1971), and others will be given here.

ON1. This is a Type I OH source according to the classification of Turner (1969). Within the limit of 5 f.u. no continuum source has been observed. Knowles *et al.* (1969) discovered H_2O emission from ON 1 at 1.35 cm. The position of the OH emission at

$$20^h08^m09^s.8 \pm 0^s.5; 31°22'41'' \pm 15'' \text{ (1950.0)}$$

(Hardebeck, 1972) agrees within the observational errors with the position found for the H_2O source. Winnberg (1970) has reported the ON 1 source to be variable.

ON2. Gehrz *et al.* (1970) suggested that this source was associated with the red star BC Cygni. However, ON2 is a mainline OH emitter and BC Cygni is not a late M-type Mira variable. Furthermore, Hardebeck has measured the position of ON2 to be

$$20^h19^m51^s.9 \pm 0^s.4; 37°17'02'' \pm 15'' \text{ (1950.0)}$$

i.e., it is situated at the edge of a H II region mapped by Higgs *et al.* (1964). In paper C of this thesis it is shown that ON2 is variable.

ON3. This source has its main emission at 1720 MHz. It is not a typical class II (*a*) source, however, as it is nearly 100% circularly polarized. Hardebeck (1971) has shown that ON3 coincides with the compact unidentified source C in the 2695 MHz continuum map published by Wynn-Williams (1969). The accurate position of ON3 is (Hardebeck, 1971)

$19^h59^m59^s.3 \pm 0^s.9; 33°26'02'' \pm 13''$ (1950.0)

ON4. This is a type II (*b*) OH source. Hardebeck (1972) measured the position of the ON4 to be

$20^h26^m40^s; 38°57'.0$ (1950.0)

Neugebauer and Becklin (Wilson and Barret, 1972) detected a weak IR star at this position. However, the IR properties of ON4 appear to be much different from those of the IR/OH stars, possibly indicating a new type of OH/IR source.

PAPER B

Searches for Microwave Spectral Line Radiation from Some Molecules in the Interstellar Space

This paper describes some of the results obtained at Onsala Space Observatory in a number of searches for microwave radiation from different molecules in several galactic radio sources. The molecules, both organic and inorganic, include OH (the vibrationally excited $^2\Pi_{3/2}, J=3/2$; $v=1$ state; and the second and third harmonics of some of ground state transitions), CH (the $^2\Pi_{1/2}$, $J=1/2$ and the $^2\Pi_{3/2}, J=3/2$ excited state), SO_2, HCN, H_2CS, NH_2CHO and CH_3CHO.

Most of the spectral lines looked for have reasonably well determined frequencies, obtained either from reported laboratory measurements or, in a few cases, calculated from molecular constants given in the literature. In all searches the frequency ranges covered were large enough to include the estimated errors in the measured or computed frequencies.

The observations were made with the 25.6 m Cassegrainian radio telescope equipped with travelling wave maser radiometers at the appropriate frequencies. The back end of the receiver consisted of two 100-channel filter receivers with individual channel bandwidths of 1 and 10 kHz.

All searches gave negative results, with the possible exception of H_2CS in W51, the observed absorption spectrum of which (obtained after 52 hours of integration time against W51) is plotted and compared with the emission profiles of the 140.8 GHz ortho-H_2CO line, $2_{12} \rightarrow 1_{11}$, and the 147.0 GHz, $J=3 \rightarrow 2$ transition in CS observed by Thaddeus *et al.* (1971) and Penzias *et al.* (1971), respectively. Details of the observations are tabulated in paper B and summarized below.

Table III. Summary of searched microwave molecular lines

Molecule	State	Rest frequency (MHz)	Sources, searched	Sensitivity (°K)
OH	Harmonics of $^2\Pi_{3/2}, J=3/2$	3330.802 3334.716 4836.693	W3(OH), W49, W75, NML Cyg.	0.02
OH	Vibrationally excited $^2\Pi_{3/2}, J=3/2$, v=1	1489.05 1536.79 1538.96 (1586.70)	NML Cyg. W3 (OH)	0.006
CH	$^2\Pi_{1/2}, J=1/2$	3362–3384 (?)	Cas A, DR21, Orion A Sgr B2, W51	0.03
CH	$^2\Pi_{3/2}, J=3/2$	4765–4773 (?)	W3 (cont)	0.03
Sulphur dioxide, SO_2	$1_{10}-1_{11}$	1518.14	W3 (cont), W3 (OH), W51	0.008
Hydrogen cyanide, HCN	$J=4, F=4-4$, $3-3, 5-5$	4488.4	Cyg A, DR21, NGC 2024, ON3, Sgr B2, W3 (cont), W3 (OH), W43, W51	0.03
Thioformaldehyde, H_2CS	$1_{10}-1_{11}$	1046.48	Cyg A, DR21, M8, ON4, Orion A, Sgr A, W3 (cont), W4, W5, W12, W44, W51, W67	0.006
	$2_{12}-2_{11}$	3139.38	DR21, Orion A, W3 (cont), W51	0.011
Formamide, NH_2CHO	$1_{10}-1_{11}$ $F=2-2, F=1-1$	1539.82 1538.08	W3 (cont), W51	0.007
Acetaldehyde, CH_3CHO	$(1_{11}-1_{10})_A$	1065.1	DR21, W3, W51	0.02

PAPER C

High Resolution Spectra of Some Strong Galactic OH Emission Sources

The very long baseline interferometer observations done so far reveal the bright Doppler features in the spectra of the galactic OH emission sources to be separate, very small, masering OH clouds. (Moran *et al.*, 1968). Single antenna high frequency resolution measurements combined with a decomposition of the observed spectra into Gaussian components are therefore a useful guide for these complicated observations. In paper C eight strong class I and II OH emission sources have been analyzed with the high frequency-resolution of 250 Hz. Some of the sources have recently been observed with VLBI techniques and the Onsala-Green Bank-Haystack baselines.

Many OH emission sources, both main line and class II sources, have been reported to vary in intensity. Observations with high signal to noise ratio and high frequency resolution would therefore offer an improved ability to detect variations in intensity as well as half-power-width and radial velocity. Some of the models suggested for the emitting OH cloud result in a velocity change observable over a few years. Furthermore, it is easy to show that for an unsaturated masering cloud with a Gaussian velocity distribution of the OH molecules the observed line shape should be exponential Gaussian with a line width proportional to (the gain factor of the cloud)$^{-1/2}$. An intensity variation would therefore be followed by a change in the width, which, although small, might be observable.

The main points of paper C can be summarized as follows:

1. The measurements were made with the Onsala 84-foot (25.6 m) radio telescope, equipped with maser amplifier and computer controlled multichannel receiver.

2. The receiver was frequency-switched and a new method was used to subtract the zero line which improves the efficiency of the system by about 75%. Furthermore, the spectrum was automatically moved an integral number of filter channels in three steps, thus reducing calibration errors and errors due to the individual filter characteristics. Since only forty 250 Hz filters were available, the observed spectrum, in some cases, consists of six to seven added observations with different center frequencies.

Table IV. Summary of observed high resolution spectra

Source	Position (1950.0) RA δ	Transition (MHz)	Polarization	Number of components	Total integrated flux ($Wm^{-2} \cdot 10^{-22}$)
W3 OH	$02^h23^m17^s$;61° 38′ 54″	1665	RC	15	128
			LC	12	122
		1667	RC	5	3
			LC	5	8
ON 2	$20^h19^m52^s$; 37° 17′ 02″	1665	RC	9	15
W75A	$20^h37^m15^s$; 42° 12′ 09″	1665	RC	5	10
			LC	6	23
W75B	$20^h36^m50^s$; 42° 26′ 58″	1665	RC	10	27
			LC	8	13
W49	$19^h07^m50^s$; 09° 01′ 24″				
	$19^h07^m58^s$; 08° 59′ 58″	1720	LC	4	36
NML Cyg	$20^h44^m34^s$; 39° 55′ 56″	1612	RC	—	780
			LC	—	780
R Aql.	$19^h03^m58^s$; 08° 09.1′	1612	RC	4	22
			LC	4	22
W51	$19^h21^m26^s$; 14° 24′ 39″	1665	RC	8	38
			LC	10	55

3. The model used in the Gaussian analysis represents the emission spectrum as an incoherent superposition of right and left circularly polarized features, each with a Gaussian velocity distribution. The method reported by Kaper *et al.* (1966) was used in the Gaussian analysis program written for the IBM 360/65 computer at the Gothenburg Universities' Computing Centre.

4. A total number of eight sources were observed. Table IV lists the sources, their positions, the frequency of the actual transition, the sense of polarization, the number of components in the spectrum, and the total integrated flux.

5. Two sources, viz. ON2 and W75B, show strong intensity variations but none of them was observed with the frequency resolution of 250 Hz on more than one occasion. No correlation between changes in intensity and line-width could therefore be seen. The variable feature in the W75B spectrum increased in intensity by a factor of 7 over seven days. However, the spectrum was not recorded continuously so it is impossible to know if it was a sudden change or a continuous flux increase over several days.

6. The most important data of the observed sources are summarized, and the measured high resolution spectra, the fitted model and the residuals are plotted. Computer-made tables are presented, listing the parameters of the individual components, the integrated flux and the corresponding kinetic

temperature of the OH molecules (assuming thermal broadening and saturated maser). Only those components that are clearly evident above noise in the data are included. The Gaussian fit is not, of course, unique and in many cases weak and wide features may consist of several narrower components.

7. The narrowest feature observed was the −43.1 km/s component in the 1667 MHz right circularly polarized emission from W3, which has a half-power width of 0.14 km/s corresponding to a kinetic temperature of 7°K. (Two narrower features are tabulated, one in the spectrum of W75B, LC, 1665 MHz and one in the spectrum of W51, RC, 1665 MHz, but they are weak uncertain components decomposed from wider features.) In no case could any significant deviation from Gaussian shape of the features be seen, thus indicating that the amplification is at least partially saturated.

PAPER D

Very Long Baseline Interferometry of Galactic OH Sources

The galactic OH emission sources turned out to be too small to be resolved by conventional interferometer techniques (Rogers *et al.*, 1967; Moran *et al.*, 1967). However, the very long baseline interferometer (VLBI) recording system, built jointly by the National Radio Astronomy Observatory and the Arecibo Ionospheric Observatory (Bare *et al.*, 1967) for work on continuum sources, could also be used to measure the structure of spectral line sources. The method was used for the first time by Moran *et al.* (1968) at MIT-Lincoln Laboratory to study the spatial structure of the strong OH spectral line emitter in the H II region named W3.

Paper D presents the result of an 18 cm spectral line VLBI observation (the third spectral line VLBI experiment and the first conducted by an observatory outside the U.S.) with a baseline 31.1×10^6 wavelengths long (maximum fringe spacing 0.0066 arc sec) between the 84-foot telescope of the Onsala Space Observatory and the 120-foot telescope of the Haystack Microwave Research Facility at MIT-Lincoln Laboratory. The measurements were performed for the following major reasons:

a) to confirm the angular sizes and spatial separations previously determined for some of the strongest and smallest W3 components;

b) to look for possible temporal variations in sizes and relative positions;

c) to obtain more information about the complex structure of the compound components; and

d) to search for fringes from a few weaker OH sources.

The recording terminal at Onsala was borrowed from the National Radio Astronomy Observatory, and the data processing was performed by means of the general purpose computer program system described in paper E. The Onsala to Haystack interferometer parameters are given in table V.

The main points of paper D are:

1. The receiver systems at Onsala as well as at Haystack and the data reduction system used to determine the fringe amplitude, fringe phase, and fringe rate versus frequency are described.

Table V. The Onsala-Haystack radio interferometer parameters (Baseline length 5599.79 km; baseline hour angle $8^h7^m34.6^s$; baseline declination $-10.835°$)

	Onsala	Haystack
Antennas	84-ft	120-ft
Aperture efficiency at 1665 MHz	≈50%	≈25%
System noise temperature	≈40°K	≈200°K
Longitude	−11° 55′ 12.8″	71° 29′ 19.2″
Geodetic latitude	57° 23′ 36.1″	42° 37′ 23.5″
Geocentric latitude	57° 13′ 3″	42° 25′ 50″
Heights	14 m	145 m

2. The most extensive observations were made on the OH source in W3 at 1665 MHz. Measurements were performed with the wide bandwidth of 120 kHz and the narrow bandwidth of 6 kHz which yield a frequency (velocity) resolution of 4.8 kHz (0.9 km/s) and 480 Hz (90 m/s).

3. The 120 kHz observations were used to determine the angular separation between the −43.7 km/s and the −45.1 km/s features of the 1665 MHz, right circular polarized emission from W3OH by fringe-rate mapping (a method described in paper E). It was shown that the −45.1 km/s feature is located 0.8″±0.2″ west and 0.2″±0.2″ north of the −43.7 km/s component. Within the limit of error this spatial separation agrees with the separation measured by Moran *et al.* (1968), and Cooper *et al.* (1971) at shorter baseline lengths.

4. High resolution cross correlation spectra of the −45.1 km/s right circular polarized feature at 1665 MHz are presented and redrawn in figure 3 below. These spectra clearly show the presence of three spatially distinct components centered at −44.8, −45.0, and −45.3 km/s. The component at −45.3 km/s appears to be the smallest one with an angular size of about 0.005 arc sec (apparent diameter $2 \cdot 10^{14}$ cm at a distance of 2.6 kpc).

5. The −43.7 km/s feature in W3 was examined with high frequency resolution. A fringe amplitude of 0.4 was obtained at a fringe spacing of 0.007 arc sec in good agreement with the previously measured size of 0.005 arc sec.

6. In total six strong OH sources were observed, including W3, W49, W51, NML Cygnus, W75A, and W75B. Only W3 and probably W49 at 1667 MHz, gave fringes. This clearly shows the need for extended VLBI observations of OH sources with moderate baseline lengths (around 1000 km). Such measurements were impossible in Europe in 1969. However, the Mark II VLBI system now being developed at the Onsala Space Observatory will allow measurements between two or more stations in Europe.

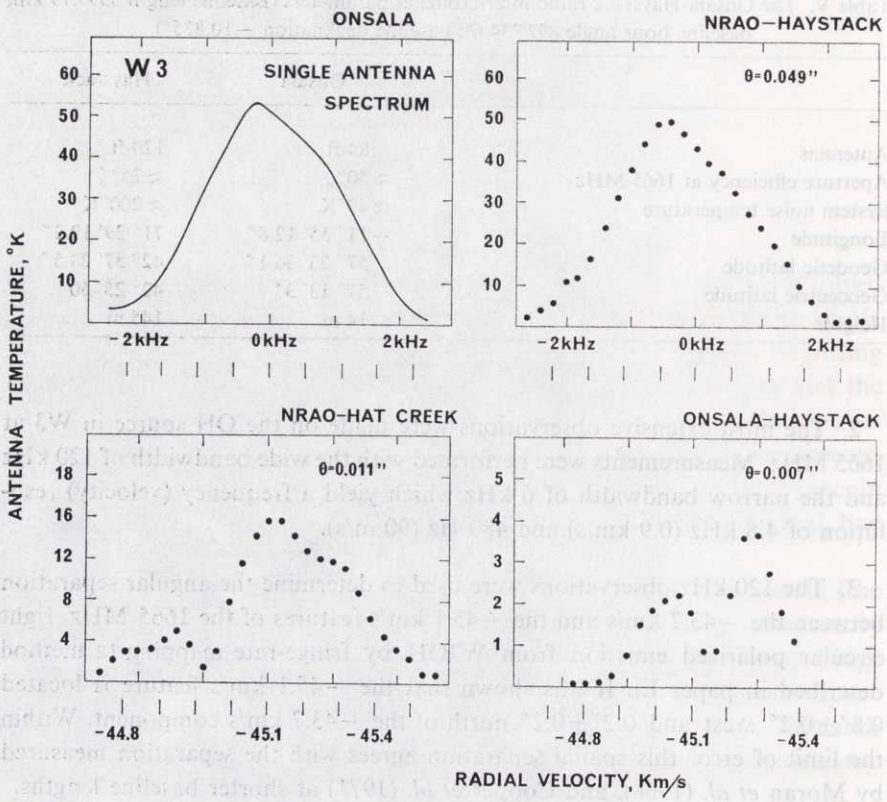

Fig. 3. An example of the high resolution spectra obtained on the −45.1 km/s right circularly polarized feature of W3(OH) at 1665 MHz for different baselines up to a length of 31×10^6 wavelengths (fringe spacing 0.007 arc sec). The integration time is 160 seconds (1800 seconds for the total power spectrum). The frequency resolution is 480 Hz (250 Hz for the total power spectrum).

PAPER E

On the Theory, Techniques, and Data Processing of Very Long Baseline Interferometry

The very long baseline interferometer (VLBI) is the most powerful instrument as to resolution. By means of the VLBI techniques developed by two groups in the U.S. and in Canada in 1967, a method is available which yields unlimited resolution for studying compact galactic and extragalactic radio sources, and which has at the same time applications in many other fields (see Introduction).

The first intercontinental VLBI experiments were performed in 1968 between CTH (Onsala Space Observatory), NRAO (Green Bank), MIT-Lincoln Lab. (Haystack), Caltech (Owens Valley Radio Observatory) and Univ. of California (Hat Creek). The data reduction of these successful measurements (Kellermann *et al.*, 1968, Moran *et al.*, 1968) was made in the U.S. Two data reduction systems had been developed; one at NRAO for continuum source observations and one at MIT-Lincoln Lab. for spectral line VLBI. The third system, usable for spectral line as well as continuum source measurements, was then developed at the Onsala Observatory to run European and intercontinental VLBI experiments.

Paper E serves as a documentation or handbook of the complicated VLBI techniques. It can be divided into three parts, dealing with VLB interferometer theory, theoretical analysis of the VLBI receiver system, and a description of the "back-end" receiver which has been developed. Many formulae given in the theoretical part of paper E are well-known and have been reported elsewhere but are included for the sake of completeness. The "back-end" receiver described, i.e. the tape synchronizer, filters, delay lines, cross-correlator, nonlinear synchronous detectors, integrators and Fourier transformer, is a soft-ware system realized by means of an IBM 360/65 computer.

The main points of paper E are:

1. The well-known relation between the geometrical time delay τ_g, the radio source position (δ_s, H_s) and the baseline parameters (δ_b,h_b) of the interferometer is extended to include the second order effect due to the motion of earth. It is shown that under extreme conditions the first order correction would give rise to a fringe rate offset of a few mHz. The relativistic effect, the maximum contribution of which is of the same order, is also discussed.

2. A table is presented which gives the baseline parameters of nine interferometer configurations of current interest. As of today eight of them have been used.

3. The relation between the fringe visibility and the brightness distribution of the source is derived in order to point out the assumptions and approximations necessary to obtain the well-known Fourier transform relation. It appears that the interferometer theory works only for an incoherent radiating source where the mutual coherence function $\Gamma(\xi_1, \xi_2, \tau)=0$ if $\xi_1 \neq \xi_2$.

The limited number of available baselines and the difficulty of having control over the absolute phase of the VLB interferometer make it necessary to use a simplified technique for restoring the brightness distribution. Furthermore, on the longest baselines the requirement of common visibility of the source at reasonable elevation requires that the observations be near the interferometer meridian and only a few points on the visibility versus projected baseline curve are obtained. These limitations mean that one has to assume the simplest and most feasible source distribution and adapt its parameters to the observed visibility. A number of fundamental distributions and their fringe visibilities are tabulated.

4. The actual VLBI receiver system is analysed.
If

a) the radiating source is unresolved

b) the signal consists of white noise

c) single sideband transmission is used

d) the signal is converted to video before time delay compensation

e) a rectangular bandpass filter of width B is used,

then the receiver output, the cross-correlation function, becomes

$$\rho(\tau)=\cos[\omega_0\tau_g-\varphi_1+\varphi_2+\pi B(\tau_g+\tau_i+\tau)]\frac{\sin \pi B(\tau_g+\tau_i+\tau)}{\pi B(\tau_g+\tau_i+\tau)} \quad (2)$$

where ω_0 is the local oscillator (LO) frequency and τ_i is the delay compensation. $\varphi_1-\varphi_2$ is the relative phase difference of the LO signals and is not allowed to vary more than a few degrees over the actual integration time. Relation (2) demonstrates that the fringe amplitude cannot be estimated by taking the peak amplitude of the cross-correlation function. A synchronous detection has to be done before integration.

The truncation of the time delay τ_i to an integral number of bits will affect the fringe phase versus frequency as well as the fringe amplitude. This effect is discussed.

5. The sensitivity of the cross-correlator interferometer is discussed. The rms errors in fringe amplitude and fringe phase are derived and compared with the corresponding relations for the total power and the correlation receivers.

6. The normalized complex cross-power spectrum (=fringe visibility versus frequency) is given by

$$S(f)=\sqrt{\frac{(T_{A1}+T_{S1})\,(T_{A2}+T_{S2})}{T_{A1}\cdot T_{A2}}}\int_{-\infty}^{\infty} R(\tau)\cdot e^{-j2\pi f\tau}d\tau \qquad (3)$$

where $R(\tau)$ is the cross-correlation function and $T_{A1}+T_{S1}$, $T_{A2}+T_{S2}$ are the single antenna signal+noise power at stations 1 and 2, respectively. The measured quantity $R_m(\tau)$ is a sample function of a random process and its statistical average approximates $R(\tau)$. Furthermore, the integration interval of relation (3) must be made finite, which determines the number of independent values of the cross-power spectrum. The equivalent filter curves for uniform and cosine weighting of $R_m(\tau)$ are given and the corresponding equivalent noise bandwidths are calculated.

7. The NRAO Mark I VLBI recording terminals use commercial digital tape recorders and the signal is one-bit digitized (infinitely clipped) before recording. The "back-end" receiver (the data processor) therefore makes use of the one-bit correlation method of spectral analysis.

It is well-known that in the non-clipped case a higher sampling rate than 2B, where B is the signal bandwidth, cannot improve the spectral estimate. However, in the clipped case a higher sampling rate does decrease the spectral variance, as the power spectrum of the clipped signal will be spread out. The decrease in signal to noise ratio due to the clipping is given by

$$\frac{\pi}{2}\,[B\int_{-B}^{B} S_S^2\,(f)df]^{1/2} \qquad (4)$$

where S_S is the spectrum of the clipped and sampled signal. Relation (4) has been tabulated for sampling rates from 2B to infinity. One notices that very little improvement is obtained by increasing the sampling rate above 4B.

8. The efficiency of a two-element interferometer is normally defined by means of the fringe spacing. However, it is evident that from a single measurement only the quantities $\int T_B(\xi)\,d\xi$ and $\int \xi T_B(\xi)\,d\xi$ can be determined.

An alternative method of mapping a source is obtained by accurate measurement of the fringe rate and time delay offsets between separate components.

It is shown that time delay mapping gives the resolution $\Delta\theta_\tau = C_\tau \cdot \dfrac{1}{B/f_0\sqrt{u^2+v^2}}$ (5)

where C_τ is a constant, f_0 is the local oscillator frequency and u, v are the spatial frequency components

$$u = \frac{D}{\lambda} \cos \delta_b \sin (H_s - h_b) \tag{6}$$

$$v = \frac{D}{\lambda} [\sin \delta_b \cos \delta_s - \cos \delta_b \sin \delta_s \cos (h_b - H_s)] \tag{7}$$

The angular resolution obtained from fringe rate mapping becomes

$$\Delta\theta_f = C_f \frac{1}{\Omega T_i \sqrt{f_x^2 + f_y^2}} \tag{8}$$

where Ω is the angular velocity of the earth, T_i is the integration time, and

$$f_x = \frac{D}{\lambda} \cos \delta_b \cos (H_s - h_b) \tag{9}$$

$$f_y = \frac{D}{\lambda} \cos \delta_b \sin \delta_s \sin (H_s - h_b) \tag{10}$$

The two methods are discussed and their capabilities are compared for various receiver systems.

9. While fringe rate mapping is limited by the phase stability of the receiver, time delay mapping is limited only by the frequency band which can be recorded. However, a very broad bandwidth can be synthesized by recording several narrow frequency bands spaced in a sequence which is like a geometrical progression. This method is analysed and an example of synthesized delay resolution function is shown.

10. The Onsala VLBI receiver, including the rubidium time and frequency standard, LO chain, and the NRAO tape recorder, is described. A block diagram of the receiver is shown in figure 4.

11. The VLBI data processor is described. It consists of a computer software system which can be run either as an autocorrelation spectral line receiver or as a crosscorrelation spectral line receiver. The total system consists of a main program (listed in paper E), twelve FORTRAN subroutines (for the mathematical calculations), and five Assembler subroutines. Some illustrating examples of the processor output are shown.

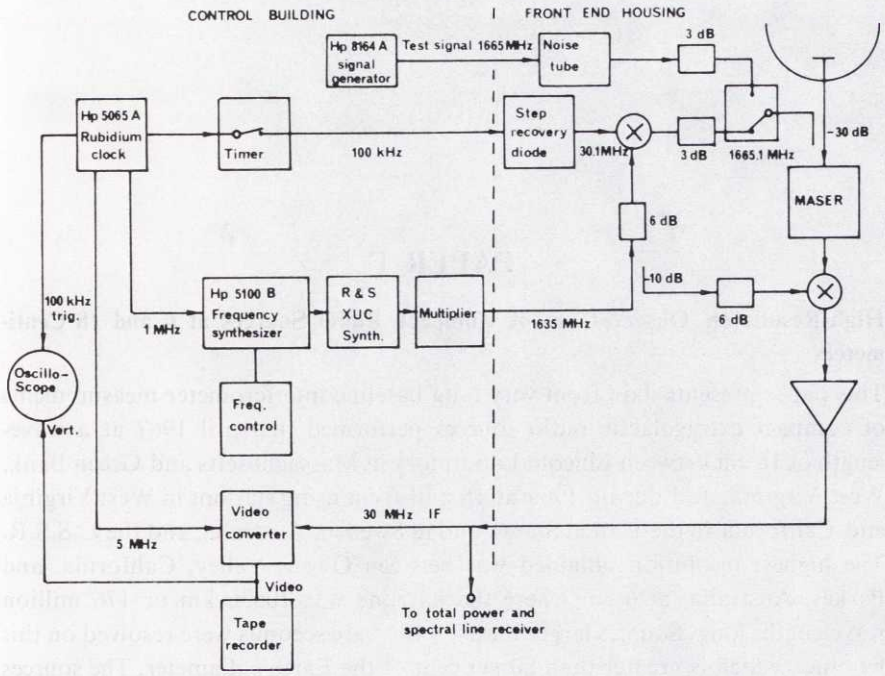

Fig. 4. Block diagram of the VLBI receiver including phase calibration system.

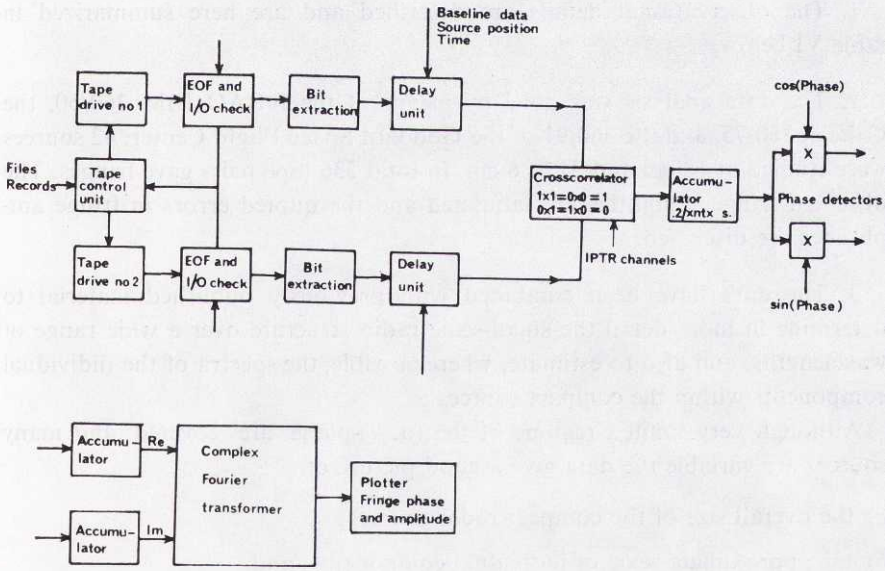

Fig. 5. Block diagram of the Mark I VLBI data processor.

PAPER F

High-Resolution Observations of Compact Radio Sources at 6 and 18 Centimeters

This paper presents data from very long baseline interferometer measurements of compact extragalactic radio sources performed in April 1967 at a wavelength of 18 cm between Lincoln Laboratory in Massachusetts and Green Bank, West Virginia, and during 1969 at 18 and 6 cm using stations in West Virginia and California in the United States, and in Sweden, Australia, and the U.S.S.R. The highest resolution obtained was between Owens Valley, California, and Parkes, Australia, at 6 cm where the baseline was 10536 km or 176 million wavelengths long. Sources larger than 4×10^{-4} arc seconds were resolved on this baseline, which is greater than 80 per cent of the Earth's diameter. The sources studied include identified QSOs and radio galaxies as well as some unidentified sources.

The main points of this paper can be summarized as follows:

1. The observational details are described and are here summarized in table VI below.

2. The data analysis was done by means of the NRAO IBM 360/50, the Caltech 360/75, and the 360/91 of the Goddard Space Flight Center. 42 sources were studied at 18 cm and 31 at 6 cm. In total 336 tape pairs gave fringes. The observed fringe visibilities are tabulated and the quoted errors in fringe amplitudes are discussed.

3. The data have been combined with previously published material to determine in more detail the small-scale radio structure over a wide range of wavelengths, and also to estimate, where possible, the spectra of the individual components within the compact sources.

Although very limited regions of the (u, v)-plane are covered and many sources are variable the data give a good picture of

a) the overall size of the compact radio sources,

b) the approximate scale of individual components, and

c) the general dependence of the structure on wavelength.

Table VI. Instrumentation and interferometer baselines.

Station	Antenna size, (m)	λ (cm)	Front end receiver	System noise, (°K)	Freq. standard
Green Bank (GB)	42	18	paramp	200	H maser
					or
	42	6	paramp	110	Rb stand.
Lincoln Lab					
Haystack (HSK)	37	18	paramp	200	H maser
Millstone (MS)	26	18	paramp	200	H maser
Owens Valley (OVRO)	40	18	paramp	250	Rb stand.
	40	6	paramp	150	Rb stand.
Parkes (PKS)	65	6	paramp	130	Rb stand.
Onsala (ONS)	26	18	maser	40	Rb stand.
		6	maser	50	Rb stand.
Crimea (CAO)	22	6	paramp	130	Rb stand.
Hat Creek (HC)	26	18	paramp	200	Rb stand.

Baseline	λ (cm)	Separation (km)	Separation ($10^6\lambda$)	Dates
GB-HSK	18	845	4.7	1967 July, Aug.
GB-MS	18	845	4.7	1968 April
GB-HC	18	3 500	19.4	1967 Aug.
GB-ONS	18	6 319	35.1	1968 Jan., 1969 April
	6	6 319	105	1968 Feb., 1969 Jan.
GB-OVRO	6	3 324	55.5	1969 Jan., March, April, May
OVRO-ONS	6	7 914	132	1969 Febr.
OVRO-PKS	6	10 536	176	1969 April
GB-CAO	6	8 035	134	1969 Oct.

4. The data, and previously published work at lower resolution, show that there is a continuous range of scale in extragalactic sources down to angular dimensions of 0.″0004 or less. If the quasi-stellar sources are assumed to be at cosmological distances, then the typical linear dimensions of the smallest components are of the order of a few parsecs or less. The unresolved component in 3C 273 is smaller than 1 pc.

5. The observed peak brightness temperatures range up to a value of about 10^{12}°K, which is the limiting brightness temperature that can occur in an opaque incoherent synchrotron source (Kellermann and Pauliny-Toth, 1969).

6. With the synchrotron model to interpret the measured angular size and cut-off frequency the magnetic strengths are estimated in the usual way, to be in the vicinity of 10^{-4} gauss in most of the resolved opaque components.

7. It is shown that, in general, the apparent angular dimensions of a source are smaller at shorter wavelengths. Five arguments are given for why it is believed that this could not be due to interstellar scattering. The results are most simply interpreted as due to the higher self-absorption cut-off frequency in the smaller components.

8. A total of twelve sources gave fringes on the longest baseline, $176 \times 10^6 \lambda$, between California and Australia. These sources all contain significant structure on a scale of 0."0005. Several sources including 0106+01, 3C 273, 3C 279, 1555+00, 2145+06, 3C 345, 3C 454.3, and 2345−16 have unresolved components which are 0."0004 or less in extent, and observations at higher resolution are necessary to study them.

9. It is shown that all opaque synchrotron sources can be resolved by using baselines restricted to the surface of the earth if the observations are made at the wavelength of maximum flux density.

10. Most of the variable sources observed were too small to be resolved with the baselines used in these measurements. One exception is the relatively nearby radio galaxy NGC 1275 (3C 84). 3C 84 was resolved on the Green Bank-Onsala baseline in both the 1968 and 1969 measurements. The fringe visibility appears to have significantly decreased during the one year between the two sets of observations, indicating an increase in angular size during this time.

With the redshift $z=0.018$ and the Hubble constant $H=100\ \mathrm{kms}^{-1}\ \mathrm{Mpc}^{-1}$ the distance to 3C84 is 54 Mpc, which means that the diameter increased from 1.4 ± 0.2 lt-yr in 1968. 0 to 2.1 ± 0.2 lt-yr in 1969.0, i.e. an expansion velocity $v/c = 0.35 \pm 0.15$ is measured. Accordingly, the variable component must be younger than the ten years previously assumed.

The unambiguous resolution of variable source components would permit a direct test of the expanding source model (Shklovskij, 1965) and allow the rate of expansion to be determined. It would also be possible to calculate the rate of change of the magnetic field strength and, in the case of identified sources whose distances are known, the total energy content. Also, for the identified variable sources it would be possible to test the hypothesis that the apparent expansion velocity is greater than that given by usual light-travel-time arguments (e.g., Rees, 1968).

A project for studying variable sources is in progress with the Onsala-Green Bank and Onsala-Owens Valley baselines.

PAPER G

Transient Wave Propagation in Inhomogeneous Ionized Media

Approximative methods for calculating the distortion of a signal after it has propagated through a dispersive medium were developed many years ago by Sommerfeld (1914) and Brillouin (1914). They used stationary phase and saddle point principles in order to determine the signal distortion and discuss the difference between group and signal velocities. They also gave an expression for the "forerunner", i.e. an expression for the initial oscillations of the wave front. A similar method may also be used to obtain the transient response of an inhomogeneous medium if one knows the phase versus frequency of the actual wave. By means of Fourier transform techniques and Taylor expansion of the phase about the signal frequency Rydbeck (1942) determined the shape of a square pulse and a sinusoidal modulated wave-train after reflection in the ionosphere. This method cannot be used at a carrier frequency near or at the penetration frequency of an ionospheric layer.

The more liberal availability of digital computers has caused an increasing interest in transient wave propagation during the past ten years. Many papers (Chen, 1963; Knop, 1964; Case, 1965) have been published presenting numerical solutions of the initial arrival and build-up of waves in homogeneous plasmas or wave guides.

The primary purpose of the investigation reported in paper G was to find exact transient wave solutions for lossless, isotropic, stratified, ionized media. Three different layers are studied, viz. the semi-infinite homogeneous medium, the exponential medium, and the symmetrical Epstein layer. Analytic expressions for the time variation of the electric field and the magnetic field caused by an incident plane unit step wave have been obtained. These wave responses can be found from the linearized wave equation,

$$\frac{\partial^2 E}{\partial z^2} - \frac{1}{c_0^2}\left(\frac{\partial^2}{\partial t^2} + \omega_p^2\right) E = 0, \tag{11}$$

(ω_p is the angular plasma frequency), from the boundary conditions far below and high up in the media, and by the use of suitable Laplace transforms. The unit step wave responses are remarkably simple mathematical expressions. Consequently, one can easily study the propagation properties of the media

and also determine the unit step modulated carrier responses which makes it possible to study, among other things, the interesting case of signal distortion and signal time delay at tunnel transmission through an ionized barrier.

1. *The semi-infinite homogeneous, ionized medium*

The transient response of this medium has been given earlier by several authors (Chen, 1963; Knop, 1964; Case, 1965; Schmidt, 1964). However, this simple case is included in paper G as an instructive introduction to the more complicated inhomogeneous cases. It is shown that the reflected and transmitted waves, if one assumes an incident unit step wave $E_I = U(t-\tau)$, can be written as

$$E_R(t,z) = \{-1 + J_0[\omega_0(t+\tau)] + J_2[\omega_0(t+\tau)]\}\ U(t+\tau) \tag{12}$$

and

$$E_T(t,z) = \{J_0[\omega_0\sqrt{t^2-\tau^2}] + \frac{t-\tau}{t+\tau} J_2[\omega_0\sqrt{t^2-\tau^2}]\}\ U(t-\tau) \tag{13}$$

where $\tau = z/c_0$.

The unit step modulated carrier response is more complicated as the Laplace transform of the electric field has two branch points and two poles in the p-plane. It is shown that the reflected and transmitted waves can be written as linear combinations of two Lommel functions of two variables. These Lommel functions have been tabulated by Dekanosidze (1956) and figures showing the initial oscillations of the transmitted electric field when the signal frequency equals the plasma frequency are presented.

2. *Ionized medium with exponential electron density profile*

It is shown that a unit step wave defined as $E = U(t-z/c_0)$ propagating into an ionized layer with its plasma frequency varying as

$$\omega_p^2 = \omega_0^2\ e^{z/H}$$

will be distorted according to

$$E_T(t,z) = J_0\left[\frac{2H}{c_0}\omega_p(z)\sqrt{e^T-1}\right] U(t-\tau \tag{14}$$

where T is given by equation (18).

This unit step wave response has a very simple mathematical form compared to the corresponding stationary solution (equation 4.30 in paper G).

Relation (14) is fundamental as it yields the complete propagation properties of the medium (see paragraph 4.3 in paper G) and besides, as a method of analysing or probing the medium by means of impulse or step wave formed test waves. At the same time it leads through convolution integrals to the medium responses for other types of incident waves. In paragraph 4.4 of paper G examples are given which show the unit step modulated carrier response of the exponentially ionized medium at three different heights.

3. *Symmetric, ionized Epstein layer (sech²-profile).*

The height variation of the electron density is given by

$$N(z) = N_m \frac{1}{\cosh^2 z/2H} \qquad (15)$$

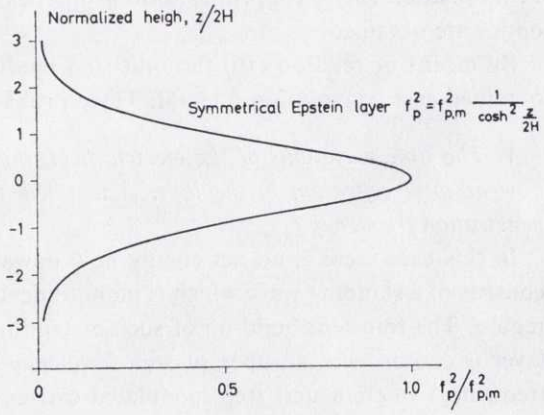

Fig. 6. The symmetrical Epstein layer.

Then the linearized wave equation can be transformed into a hypergeometric differential equation and the unit step wave response can be obtained by means of the Laplace transforms derived in appendix 1 of paper G as

$$E_T(t,z) = P_{\gamma-1/2}\left[1 + \frac{2}{1+e^{-z/H}}(e^T - 1)\right] U\ t-\tau \qquad (16)$$

where P is a Legendre function, γ is a medium scale factor given by

$$\gamma^2 = \frac{1}{4} - \frac{4H^2}{c_0^2}\omega_{p,m}^2 \qquad (17)$$

and

$$T = \frac{c_0}{2H}(t-\tau) \qquad (18)$$

By means of relation (16) wave propagation properties of the layer are studied. Far above the layer (where $z/2H \gg 1$) one obtains

$$E_T(t,z) \sim P_{\gamma-1/2}(2e^T - 1)\ U(t-\tau) \qquad (19)$$

which is the transmitted wave.

Far below the layer (where $z/H \ll -1$) one obtains

$$E_T(t,z) \sim P_{\gamma-1/2}(2e^{T_-}) \qquad [T_- = \frac{c_0}{2H}(t+\tau);\ T \gg 1] \qquad (20)$$

which represents the reflected wave.

The quantity $2H\omega_{p,m}/c_0$ of the F-layer in the ionosphere is of the order of 10^3 and accordingly $|\gamma| \gg 1$ and γ is imaginary. The transient wave response can thus be approximated as

$$E_T(t,z) \sim A(t,z)\cos(\eta\xi - \pi/4) \qquad (21)$$

where $j\eta = \gamma$ and A and ξ are defined by equation (5.46) and (5.45) in paper G. From relation (21) wave propagation properties in agreement with geometrical optics are obtained.

By means of relation (16) the unit step modulated carrier response can be obtained as a convolution integral. Three problems are analysed, viz.

1. *The time variations of the electric field, the magnetic field and the energy flow at total reflection in the layer,* i.e. *when the signal frequency* $f_1 \ll$ *the penetration frequency* $f_{p,m}$.

In this case there is no net energy flow upwards and the steady-state wave consists of a standing wave which is monotonically decreasing in the evanescent region. The transient build-up of such a standing wave is studied. An Epstein layer is chosen with an apex plasma frequency $f_{p,m} = 5c_0/2H$ (the penetration frequency) where a unit step modulated carrier of frequency $f_1 = 1.25c_0/2H$ is the incident wave.

From the energy flow $Z_0 S_{T,\,\mathrm{sin}}$ one notices that the electromagnetic wave consists of an up-going and a returning forerunner, a transition region which often has a very deformed waveform, and the build-up region of the steady-state standing wave.

2. *Signal distortion when the carrier frequency is equal to or close to the penetration frequency of the layer.*

When the carrier frequency of a radio signal approaches the penetration frequency of an ionized barrier the wave experiences strong frequency dispersion and becomes considerably distorted.

Figure 7 (figure 5.11 a in paper G) shows the envelope of the transmitted wave for six carrier frequencies. When $\omega_1 \gg \omega_{p,m}$ the steepest portion of the leading edge agrees very well with the Fresnel integral obtained from the quasi-monochromatic theory.

However, the true envelope oscillates more slowly for large values of T. It is shown that the asymptotic expression for $E_{T,\,\mathrm{sin}}$ can be written as

$$E_{T,\,\mathrm{sin}} \sim \underbrace{C_1 \cos\left(\frac{2H}{c_0}\omega_1 T - c_1\right)}_{E_{T,\,\mathrm{stationary}}} + C_2 e^{-T/2} \cos\left(\frac{2H}{c_0}\omega_{p,m} T - c_2\right) \qquad (22)$$

$$(T \gg 1)$$

where C_1, C_2, c_1 and c_2 are constants.

Accordingly, the transmitted wave is modulated by the plasma oscillations sustained in the apex region and the amplitude of the modulation decreases with time as $e^{-T/2}$. One also notices that the modulation disappears when $\omega_1 = \omega_{p,m}$, which can be seen from figure 7.

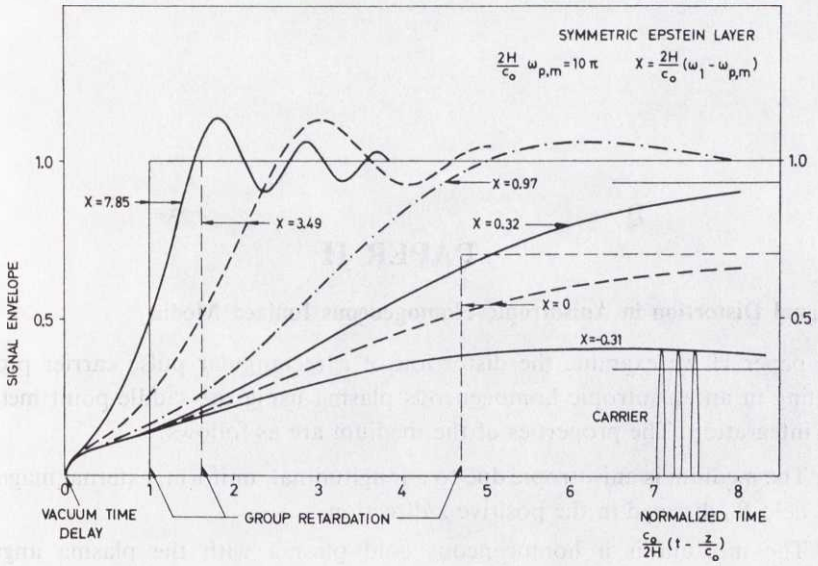

Fig. 7. The envelope of the unit step modulated carrier transmitted through a symmetrical Epstein layer with an apex plasma frequency $f_{p,\,m}=5c_0/2H$ at six different carrier frequencies.

3. *Transient response at tunnel transmission through a thin barrier.*

In order to study this interesting case the signal frequency f_1 of the step modulated carrier and the apex plasma frequency $f_{p,m}$ are chosen to be equal to 1.5 $c_0/2H$ and 1.75 $c_0/2H$, respectively. This means that the transmission factor $|T|$ obtained from

$$|T|^2=\frac{\cosh(2\pi\omega_1 2H/c_0)-1}{\cos(2\pi\gamma)+\cosh(2\pi\omega_1 2H/c_0)} \tag{23}$$

is equal to 0.007.

In the stationary state there is a negligible energy transport upwards and up to the apex level the transient wave consists of an upgoing precursor, the reflected precursor decreasing in amplitude with increasing height, and then the build-up region of the standing wave. Even above the apex of the layer there is a reflected precursor, i.e. a time interval where the net energy flow is directed downwards. Far above the layer the energy flow is of course always directed upwards. As to the group and signal velocities at tunnel transmission through the layer it is shown that there is no relation between the two. As a matter of fact it is difficult, if not impossible, to define the signal velocity, which becomes a function of the barrier form, of the carrier frequency, and also of the signal envelope used.

PAPER H

Signal Distortion in Anisotropic Homogeneous Ionized Media

In paper H we examine the distortion of a rectangular pulse carrier propagating in an anisotropic homogeneous plasma using the saddle-point method of integration. The properties of the medium are as follows:

1) The medium is anisotropic due to a longitudinal, uniform, external magnetic field B_0 directed in the positive z-direction.
2) The medium is a homogeneous cold plasma with the plasma angular frequency ω_0.
3) The collision losses are omitted.

The properties of the electromagnetic signal are:

1) The signal is a plane wave propagating in the positive z-direction (i.e., along the external magnetic field).
2) At $z=0$ the signal is linearly polarized with the electric field E in the x-direction equal to

$$E(t)_{z=0} = \sin(\omega_1 t)\, U(t) \tag{24}$$

Since the magnetic field is directed along the propagation path, two circularly polarized modes which propagate independently exist. This means that the original pulse will normally be split up into two pulses, the refractive indices for which are given by

$$n_{\pm}^2 = 1 - \frac{\omega_0^2}{\omega(\omega \pm \omega_H)} \tag{25}$$

where ω_H is the gyrofrequency. The subscripts + and − denote the counterclockwise and clockwise rotating components, respectively.

The unit step modulated sine-wave response (i.e., the transmitted field at $z>0$) can be found by means of simple transform techniques. For example, it is shown that the x-component becomes

$$E_x^t(t,z) = \mathrm{Re}\left\{ \frac{1}{2\pi} \int_{-\infty - jc}^{\infty - jc} \frac{\omega_1}{\omega_1^2 - \omega^2} e^{j\omega(t - n_+ z/c_0)}\, d\omega \right\} \tag{26}$$

The main purpose of paper G was to find asymptotic expressions for this relation suitable for numerical calculations.

The "Sommerfeld precursor" (Sommerfeld, 1914), i.e., the initial oscillations of the transmitted signal, is obtained by distorting the integration contour into a large semicircle in the lower half of the complex ω-plane. One obtains

$$E_x'(t,z) \sim \frac{2\omega_1}{\omega_0}\left[\frac{t-z/c_0}{2z/c_0}\right]^{1/2} J_1\left\{\omega_0\left[\frac{2z}{c_0}\left(t-\frac{z}{c_0}\right)\right]^{1/2}\right\} U\left(t-\frac{z}{c_0}\right)$$

$$E_y'(t,z) \sim 0 \tag{27}$$

valid for $\left(t-\frac{z}{c_0}\right) \ll \left(t+\frac{z}{c_0}\right)$

i.e. the same expressions as for the isotropic case, since in the region of validity the instantaneous frequency of the signal is much larger than the gyrofrequency.

The second precursor, the leading edge of the main signal, and the posterior are obtained from (26) using the saddle-point method of integration. For instance, the following expression for the x-component of the transmitted unit step modulated carrier is obtained:

$$E_x'(t,z) = E_{x,+}'(t,z) + E_{x,-}'(t,z) \tag{28}$$

where

$$E_{x,\pm}'(t,z) \approx 1/4\{[1+S(\alpha_\pm)+C(\alpha_\pm)]\sin\gamma_\pm + [C(\alpha_\pm)-S(\alpha_\pm)]\cos\gamma_\pm\} +$$

$$+ \frac{1}{2(\omega_{s,\pm}+\omega_1)\sqrt{2\pi\omega_\pm''}} \cdot \cos(\omega_\pm + \pi/4) + f_\pm(t,z) \tag{29}$$

and

$\omega_{s,\pm}(t)$ is the positive solution to

$$\frac{d}{d\omega}\left[\omega\left(t-n_\pm\frac{z}{c_0}\right)\right]=0$$

(i.e., the positive saddle point)

$$\omega_\pm = \left[\omega\left(t-n_\pm\frac{z}{c_0}\right)\right]\omega=\omega_{s,\pm}$$

$$\omega_\pm'' = \left\{\frac{d^2}{d\omega^2}\left[\omega\left(t-n_\pm\frac{z}{c_0}\right)\right]\right\}\omega=\omega_{s,\pm}$$

$$\gamma_\pm = \omega_\pm + \frac{\pi}{2}\alpha_\pm^2$$

$$\alpha_{\pm} = \sqrt{\frac{\omega_{\pm}''}{\pi}}(\omega_1 - \omega_{s,\pm}).$$

C and S are the Fresnel integrals and

$$f_{\pm}(t,z) = \begin{cases} 0 \text{ when } \omega_{s,\pm} \geq \omega_1 \\ 1/2 \sin \omega_{1,\pm} - 1/2 \sin \gamma_{\pm} \text{ when } \omega_{s,\pm} \leq \omega_1 \end{cases}$$

$$\omega_{1,\pm} = \left[\omega\left(t - n_{\pm}\frac{z}{c_0}\right)\right]_{\omega=\omega_1}$$

The range of validity of (28) is determined by the condition

$$\omega_{\pm}'' \gg 1$$

which eliminates the immediate vicinity of the wavefront, where instead (27) is valid

From relation (28) which is the unit step modulated sine-wave response, we obtain the response of a rectangular pulse carrier of duration T as

$$E^t_{x,\,\text{pulse}}(t,z) = E^t_x(t,z) - E^t_x(t-T,z)$$

$$[\omega_1 T = 2\pi \cdot n;(n=1, 2, 3 \ldots)]. \qquad (30)$$

Numerical results obtained from (29) and (30) are shown and discussed. Here two figures are redrawn depicting the distorted envelope of a pulse carrier for two cases: $\omega_H = 0$ (the isotropic case), and $\omega_H = 0.1\ \omega_0$. In both cases the carrier frequency ω_1 is equal to $1.1\omega_0$.

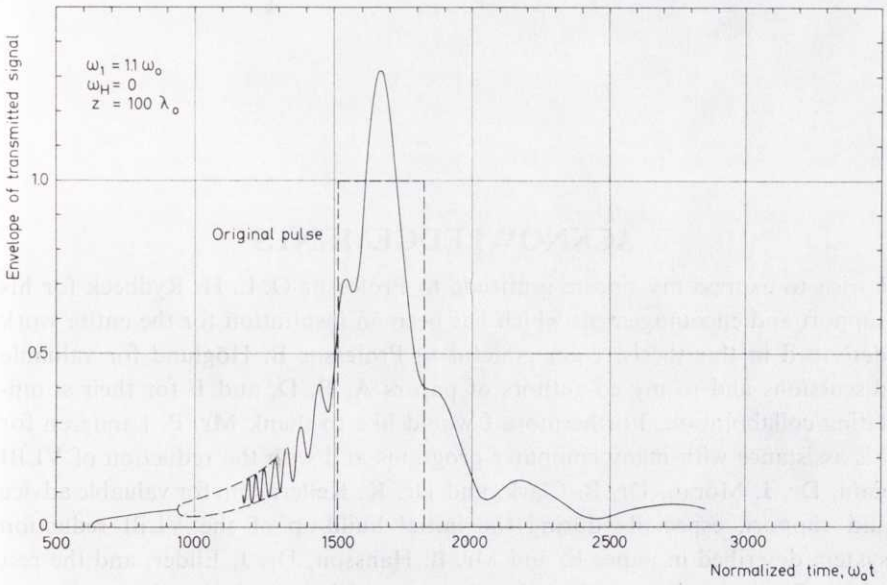

Fig. 8. The transmitted pulse at $z=100\lambda_0$ (λ_0 is the plasma wavelength). Carrier frequency $\omega_1=1.1\omega_0$. Pulse duration $T=100\pi/\omega_0=110\pi/\omega_1$. The medium is isotropic, i.e., $\omega_H=0$.

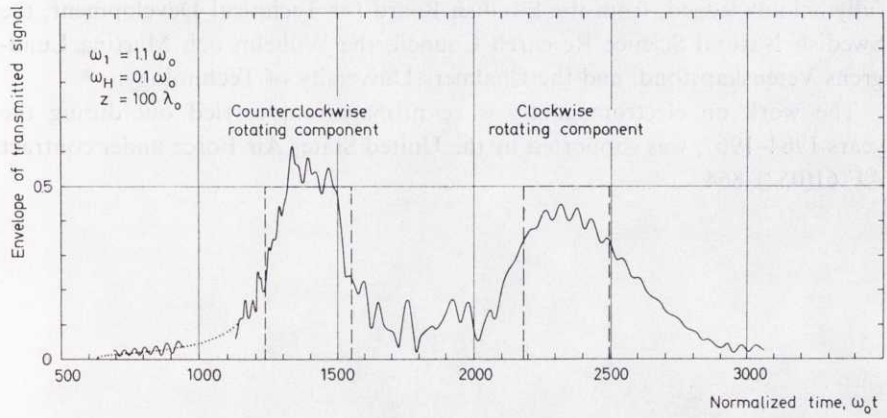

Fig. 9. The x-component of the transmitted pulse carrier at $z=100\lambda_0$. Gyrofrequency $\omega_H=0.1\omega_0$.

ACKNOWLEDGEMENTS

I wish to express my sincere gratitude to Professor O. E. H. Rydbeck for his support and encouragement which has been an inspiration for the entire work described in this thesis. I am grateful to Professor B. Höglund for valuable discussions and to my co-authors of papers A, B, D, and F for their stimulating collaboration. Furthermore I would like to thank Mr. P. Landgren for his assistance with many computer programs and with the reduction of VLBI data, Dr. J. Moran, Dr. B. Clark, and Dr. K. Kellermann for valuable advice and support, especially during the initial build-up of the VLBI reduction system described in paper E, and Mr. B. Hansson, Dr. J. Elldér, and the rest of the Onsala staff for technical assistance and help with the observations.

The discussions with Dr. J. Askne regarding electromagnetic wave distortion have been very stimulating and valuable.

I am also grateful to the National Radio Astronomy Observatory for their loan of the Mark I VLBI recording system.

The work reported in papers A–D and F would not have been possible without the excellent receivers built by Dr. E. Kollberg, Messrs. B. Hansson, C-O. Lindström, L. Andréasson, L-I. Lundahl, L-G. Gunnarsson, M. Alfredsson and Miss M. Hansen.

The radio astronomical work has been supported by grants, hereby gratefully acknowledged, from the Swedish Board for Technical Development, the Swedish Natural Science Research Council, the Wilhelm och Martina Lundgrens Vetenskapsfond, and the Chalmers University of Technology.

The work on electromagnetic wave propagation, carried out during the years 1964–1967, was supported by the United States Air Force under contract AF 61(052)–864.

REFERENCES

Bare, C., Clark, B. G., Kellermann, K. I., Cohen, M. H., Jauncey, P. L., Science, *157*, 189 (1967).

Becklin, E. E., Neugebauer, G., Ap. J., *147*, 799 (1967).

Brillouin, L., Ann. Physik, Lpz, *44*, 203 (1914).

Broten, N. W., Legg, T. H., Locke, J. L., McLeish, C. W., Richards, R. S., Chrisholm, R. M., Gush, H. P., Yen, J. L., Galt, J. A., Science, *156*, 1592 (1967).

Case, C. T., Proc. IEEE, *53*, 730 (1965).

Cerillo, M. A., M.I.T.-Res. Lab. of Electronics, Cambridge, Mass., Rept TR-55 2 a (1950).

Chen, S. N. C., Proc. IEEE (Corr), *51*, 1045 (1963).

Cooper, A. J., Davies, R. D., Booth, R. S., M.N.R.A.S., *152*, 383 (1971).

Davies, R. D., Rowson, B., Booth, R. S., Cooper, A. J., Gent, H., Adgie, R. L., Crowther, J. H., Nature, *213*, 1109 (1967).

Dekanosidze, E. N., "Tables of Lommel's functions of two variables", Pergamon Press, New York (1960).

Epstein, P. S., Proc. Nat. Acad. Sci., Wash., *16*, 627 (1930).

Gehrz, R. D., Ney, E. P., Stecker, D. W., Ap. J. Letters, *161*, L 219 (1970).

Goss, W. M., Ap. J. Suppl., *15*, 131 (1968).

Gundermann, E. J., Thesis, Harvard Univ. (1965).

Hanbury Brown, R., Ann. Rev. Astron. Ap., *6*, 13 (1968).

Hardebeck, E. G., Ap. J., *170*, 281 (1971).

Hardebeck, E. G., Ap. J., *172*, 583 (1972).

Haskell, R. E., Case, C. T., Phys. Sc. Res. Papers 241, USAF Cambridge Res. Labs. Tech. Rept. (1966).

Higgs, L. A., Broten, N. W., Medd, W. J., Raghaurao, R., M.N.R.A.S., *127*, 367 (1964).

Kaper, H. G., Smits, D. W., Schwartz, U., Takakubo, K., Woerden, H. van., B. A. N., *18*, 465 (1966).

Kellermann, K. I., Pauliny-Toth, I. I. K., Ap. J. Letters, *155*, L 71 (1969).

Kellermann, K. I., Clark, B. G., Bare, C., Rydbeck, O., Elldér, J., Hansson, B., Kollberg, E., Hoglund, B., Cohen, M. H., Jauncey, D. L., Ap. J. Letters, *153*, L 209 (1968).

Knop, C. M., Proc. IEEE (Corr), *52*, 99 (1964).

Knowles, S. H., Mayer, C. H., Sullivan III, W. T., Science, *166*, 221 (1969).

McReady, L. L., Pawsey, J. L., Payne-Scott, R., Proc. Roy. Soc. A, *190*, 357 (1947).

Michelson, A. A., Ap. J., *51*, 257 (1920).

Moran, J. M., Barret, A. H., Rogers, A. E. E., Burke, B. F., Zuckerman, B., Penfield, H., Meeks, M. L., Ap. J. Letters, *148*, L 69 (1967).

Moran, J. M., Burke, B. F., Barret, A. H., Rydbeck, O. E. H., Hansson, B., Rogers, A. E. E., Ball, J. A., Cudaback, D. D., Astron. J. (Suppl.), *73*, S108 (1968).

Moran, J. M., Burke, B. F., Barret, A. H., Rogers, A. E. E., Carter, J. C., Ball, J. A., Cudaback, D. D., Ap. J. Letters, *151*, L 99 (1968).

Neugebauer, G., Martz, D. E., Leighton, R. B., Ap. J., *142*, 399 (1965).

Penzias, A. A., Jefferts, K. B., Wilson, R. W., Ap. J. Letters, *168*, L 53 (1971).

Raimond, E., Eliasson, B., Ap. J., *150*, L 171 (1967).
Rees, M. J., Nature, *211*, 468 (1968).
Rydbeck, O., Trans. Chalmers Univ. Techn., *3* (1942).
Ryle, M., Vonberg, D. D., Proc. Roy. Soc. A, *193*, 98 (1948).
Schmidt, Proc. IEEE, *NS-11*, 125 (1964).
Schmidt, M., In Stars and Stellar Systems (ed. A. Blaauw and M. Schmidt), *5*, 513, Univ. of Chicago Press (1965).
Shklovskij, J., Astr. Zh., *42*, 30 (1965).
Sommerfeld, A., Ann. Physik, Lpz, *44*, 177 (1914).
Thaddeus, P., Wilson, R. W., Kutner, M., Penzias, A. A., Jefferts, K. B., Ap. J. Letters, *168*, L 59 (1971).
Ulrich, B. T., Neugebauer, G., McCammon, O., Leighton, R. B., Hughes, E. E., Becklin, E. E., Ap. J., *146*, 288 (1966).
van der Hulst, H. C., Nederl. Tijds. v. Natuurkunden, *11*, 201 (1945).
Weaver, H., Williams, D. R. W., Dieter, N. H., Lum, W. T., Nature, *208*, 29 (1965).
Weaver, H., Dieter, N. H., Williams, D. R. W., Ap. J. Supplement, No 146 (1968).
Weinreb, S., Barret, A. H., Meeks, M. L., Henry, J. C., Nature, *200*, 829 (1963).
Wilson, W. J., Barret, A. H., Science, *161*, 778 (1968).
Wilson, W. J., Barret, A. H., Astron. & Astrophys., *17*, 385 (1972).
Winnberg, A., Astron. & Astrophys., *9*, 259 (1970).
Wynn-Williams, C. G., Ap. J. Letters, *3*, 195 (1969).

GÖTEBORG
ELANDERS BOKTRYCKERI AKTIEBOLAG
1972